Characteristics of Combined Loading Demands on the Piers of Skewed Bridges

Nahid Attarchian[1], Afshin Kalantari[2*], and Abdolreza S. Moghadam[3]

1. Ph.D. Candidate, International Institute of Earthquake Engineering and Seismology (IIEES), Tehran, Iran
2. Assistant Professor, International Institute of Earthquake Engineering and Seismology (IIEES), Tehran, Iran, * Corresponding Author; email: a.kalantari@iiees.ac.ir
3. Assistant Professor, International Institute of Earthquake Engineering and Seismology (IIEES), Tehran, Iran

ABSTRACT

Due to the correlation of natural vibration modes of skewed bridges, and the multi-directional nature of the earthquake ground motions; piers of skewed bridges would be subjected to combined axial, flexural and torsional loadings. The characteristic of combined loading of the piers depends upon several parameters including the strong ground motion characteristics and the structural system type. In this research, seismic performance of a group of torsion sensitive skewed bridges with three different pier-deck connections is studied. Skew angles vary from 0° to 60°. Seismic performance of the bridges is investigated conducting bidirectional nonlinear time history analysis in OpenSees. Considering the effect of different pier-deck connection types, combined loading demand on the skewed piers is compared with those on the straight piers. On the basis of results, for both pinned and fixed piers, ductility demand increases with the skew angle. Opposed to pinned piers, fixed piers are subjected to combined torsional-flexural loadings, and the torsional demand increases with an increase in the skew angle. The value of torsional demand on fixed piers is limited to one half of cracking torque of the section (Tcr/2). Concerning the collapse prevention criteria, 30 degree skew angle is found to be a threshold skew angle. For bridges with skew angles greater than 30 degree, applying monolithic pier-deck connections is more sensible.

1. Introduction

According to the observations of recent earthquakes, the responses of straight bridges are significantly different from those of curved and skewed bridges [1-3]. Common behavior mode in skewed bridges is composed of transversal and longitudinal movements plus rotation about the vertical axis of the deck. This fact may lead to deck collapse or considerable residual displacements in the deck. On the other hand, extensive damage is probable in the substructure of curved and skewed bridges with monolithic pier-deck connections (Figure 1). Piers have a vital role in the seismic performance of the bridges. In order to provide the adequate capacity, force and displacement demands on the piers should be estimated properly.

Previous studies were mainly concentrated on the effect of skew angle on the seismic performance of skewed bridges. Ghobarah and Tso [5] used spine-line model to represent bridge deck and columns. They have observed coupled flexural-torsional motions of the bridge deck and excessive compression demands on columns. Meng and Lui [6]
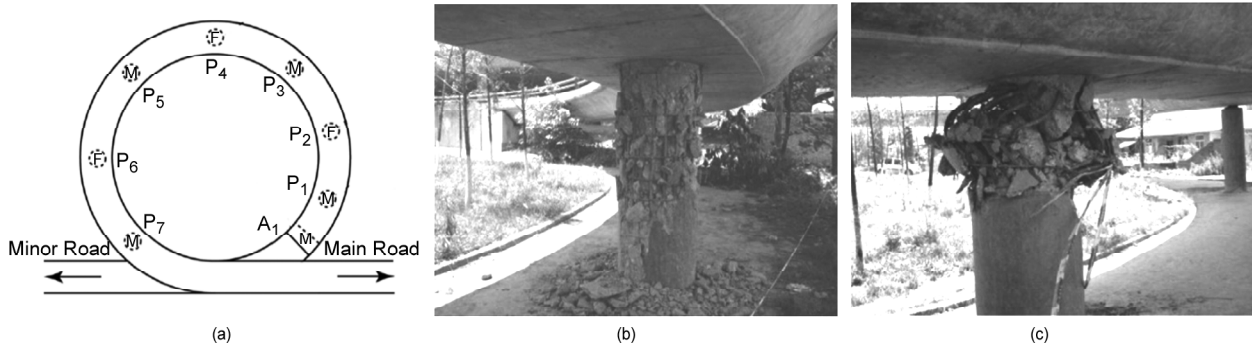
Figure 1. Shear and flexural failures in fixed piers of Huilan bridge: a) bridge plan (F: fixed connection, M: rubber bearing); b) damaged fixed P2; c) damaged fixed P4 (left), undamaged pinned P3 (right [4]).

investigated the behavior of Foothill Boulevard Undercrossing and stated that seismic performance of the bridge is strongly influenced by column boundary conditions and skew angle. Later, Mohti and Peckan [7] assessed the seismic performance of a three-span continuous box girder bridge for skew angles 0-60°. They compared finite element and beam-stick modeling approaches. Based on their studies, coupled lateral-torsional response of moderate skewed bridges could be captured via simplified beam-stick models. In a more recent study, Wilson et al. [8] have examined the effect of skew angle on the seismic performance of reinforced concrete bridges and reported that the planar rotation in the superstructure of skewed bridge induces coupled demand on the piers. Based on their findings, responses are proportional to the skew angle. They have suggested applying more rigorous modeling approach to capture complex interactions for high levels of skew angle (exceeding 30 deg.). At the same time, seismic performance of a group two-span simply supported bridges with varying skew angles subjected to a suite of bi-directional ground motions representing different hazard levels have been studied by Deepu et al. [9]. They have reported that a normal bridge suffers negligible in-plane residual rotation. However, all the skew models suffer significant (peak and residual) rotations. Besides, both transverse and longitudinal deck displacements and deck rotation increase with an increase in the skew angle.

Beside the aforementioned numerical studies, several experimental studies have been carried out on reinforced concrete bridge piers subjected to combined cyclic torsion and flexure [10-15]. These experimental tests aimed to investigate the effect of combined torsional-flexural loadings on the flexural ductility and strength of bridge piers. However, there is a considerable discrepancy among these tests concerning the assumed ratio of torsion to flexure in the sections. Therefore, investigating the behavior of skewed bridges with regards to characteristic of combined loadings in the piers has yet to be addressed.

The main objective of this research is to determine the characteristic of combined loadings in the piers of skewed bridges, with different pier-deck connections. In this study, a torsion sensitive bridge with single pier bents is modeled; the skew angles vary from 0° to 60°. The bridge has four spans with continuous deck. Three different types of pier-deck connections are applied in the considered skew angles. The numerical spine models are developed in OpenSees [16]. The models have been subjected to the bidirectional earthquake excitations. Their seismic performances have been investigated through nonlinear time history analysis. The trends in seismic responses are studied considering different skew angles and connection types. The results of this study provide a significant insight into the dynamic responses and seismic vulnerabilities of skewed bridges with different pier-deck connections, which may be utilized for future design of bridges similar to those considered in this study.

2. Characteristics of the Torsion Sensitive Bridge

Multicolumn bent bridges provide relatively larger global torsional stiffness in comparison to single-column bent bridges. Consequently, they are better choices for skewed bridges. However, in this research, in order to investigate a more crucial case relating to the rate of seismic demands on the piers, a
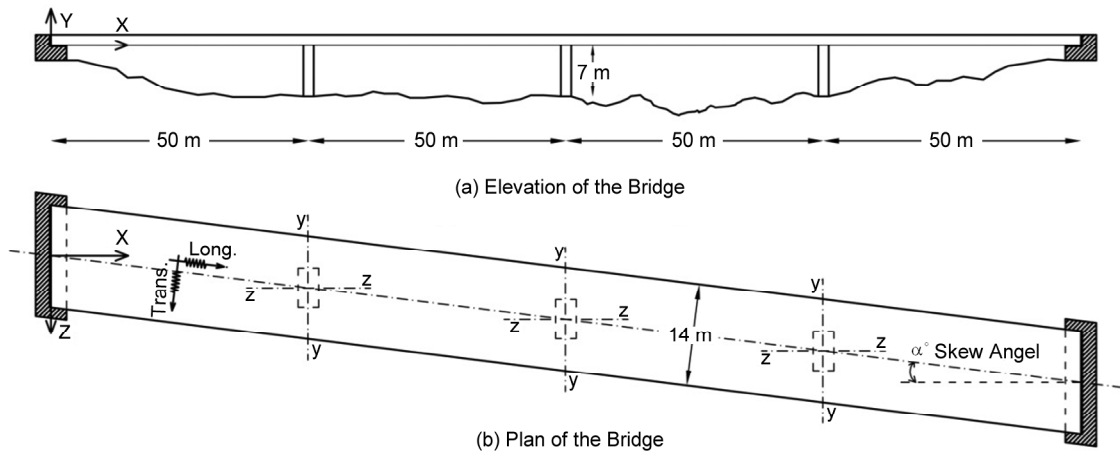
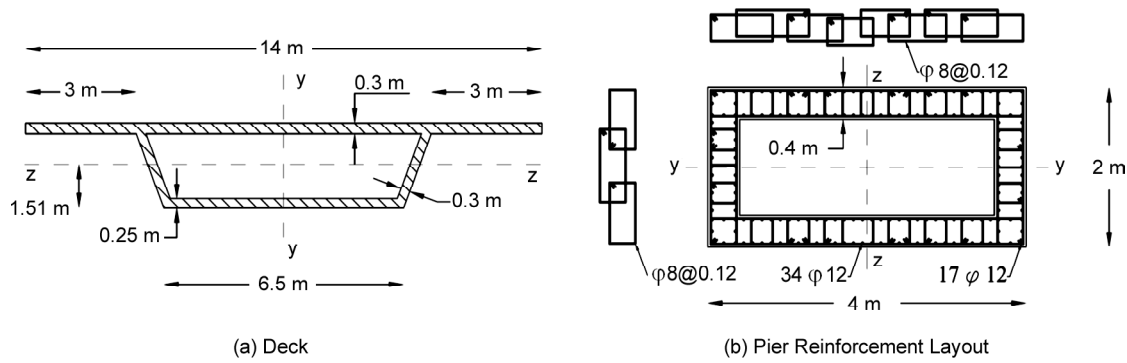**Figure 2.** General layout of the skewed bridge.

Figure 3. Cross sections of deck and piers.

single-pier bridge has been chosen as the seed bridge. Pinto et al. [17] have designed the straight bridge according to Eurocode 8 provisions [18] for PGA 0.35g. The straight layout is widely studied before by Kappos et al. [19] and Isakovic et al. [20]. Figure (2) shows the plan, elevation, global axes, and local longitudinal and transversal axes of the bridge. Cross section details of the deck and piers are shown in Figure (3). In order to compare the results, the identical pier design is applied and models are only different in the connection types and skew angles. The abutments are seat-type with bearings under the webs of box girder; and the piers are supported on spread footings. The properties of concrete are selected in accordance with C25/30 and all reinforcing bars are S500.

3. Pier-Deck Connection types

Both monolithic and seat-type pier-deck connections have already been applied in the reference bridge by Casarotti and Pinho [21] and Akbari and Maalek [22]. In the fixed or monolithic connections,

the reinforcement bars of the pier are well anchored into the deck. In the seat-type connections, deck simply rests on the bearings (fixed or sliding) and the relative rotation is free between sub- and super-structure. The schematic description of studied pier-deck connection types is presented in Figure (4).

The behavior of shear keys are considered in two extreme states: a) fully operational; b) failed. P models are seat-type bridges with fixed bearings and fully operational shear keys (pinned piers). In these connections, relative displacement between pier and deck is totally eliminated; therefore, shear forces are
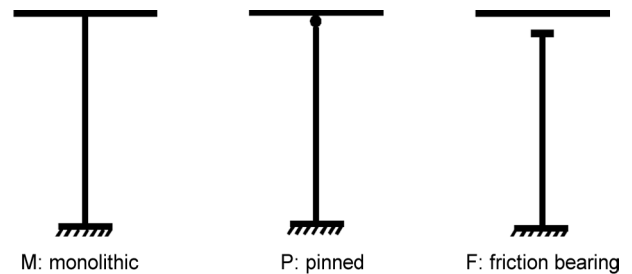

Figure 4. The schematic description of the pier-deck connections of the models.

transferred by shear keys from superstructure to the substructure. F models stand for seat-type bridges with frictional sliding bearings and ineffective internal shear keys. The sliding bearings have plate interfaces of ploytetrofluoroethylene (PTFE) and stainless steel.

4. Numerical Modeling of the Bridges

Numerical analyses are carried out in the OpenSees [16] finite element package. Figure (5) shows a typical finite element spine model of the representative skewed bridge, used in the simulations. Verified and validated modeling approaches are applied in this study based on previous works of Casarotti and Pinho [21] and Aviram et al. [23]. Details of modeling process are provided in the following.

4.1 Modeling of the Deck

The pre-stressed box girder deck is modeled via equal length linear elastic-beam-column elements. Table (1) presents the elastic properties of non-cracked cross section. In this table, E is Young's modulus (25GPa); and G is shear modulus (10 GPa). The deck element is modeled at the height of its center of gravity, 1.51 m above the pier, and

Table 1. Elastic properties of deck cross section.

EA $(10^7$ kN)	EI_y $(10^7$ kN.m^2)	EI_z $(10^7$ kN.m^2)	GJ $(10^7$ kN.m^2)
17.4	13.43	221.13	13.06

connected to the top of the pier by a rigid element (Figure 5). The distributed mass of deck elements is about 20.2 ton/m. The translational and rotational nodal masses are computed and assigned based on the above-mentioned values.

4.2. Modeling and Verifying the Cyclic Behaviour of the Piers

Regarding the combined loading of the piers, a modeling technique should be applied to account for the interaction between loads. The integrated fiber section modeling via nonlinear beam-column ele-ments can inherently accounts for geometric nonlinearity, material inelasticity, and interaction between moments and axial load. Torsional and shear behaviors are modeled by uniaxial elastic materials and are aggregated with the fiber section element. According to Caltrans [24], torsional stiffness of piers is reduced to $0.2J_c$ concerning the initial cracking of the piers in torsion. The piers are modeled via three equal length force based nonlin-
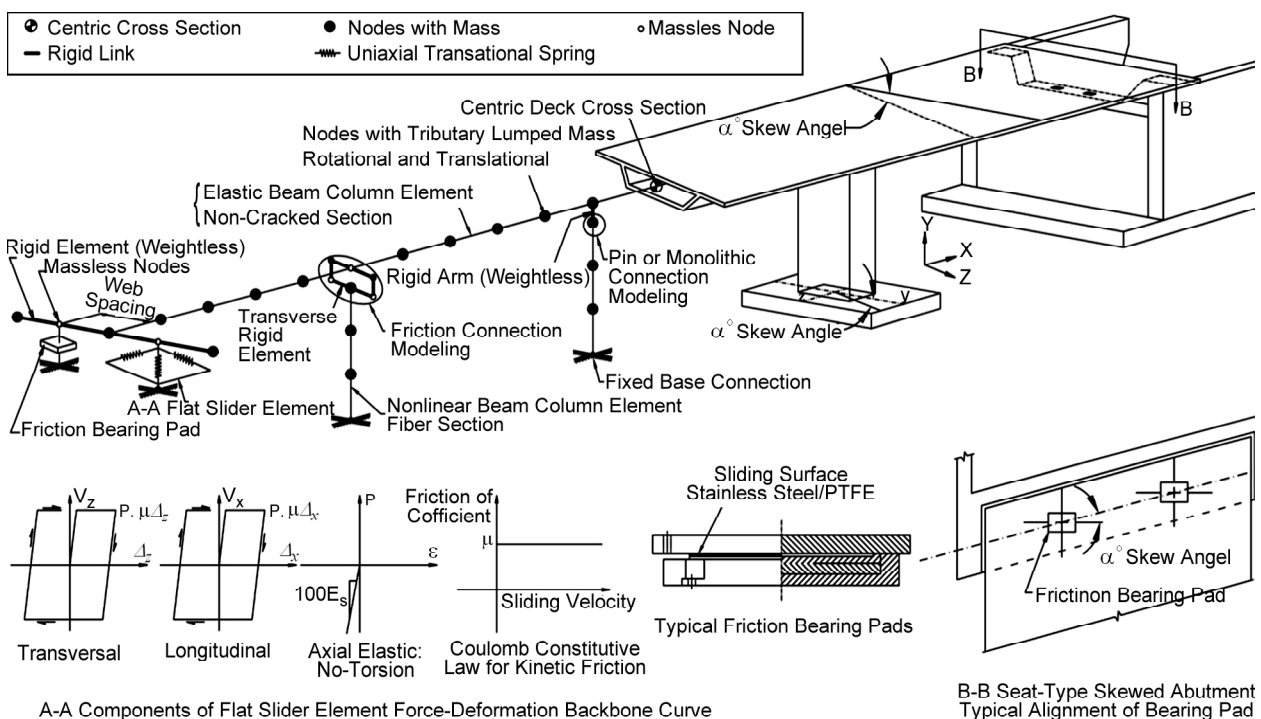

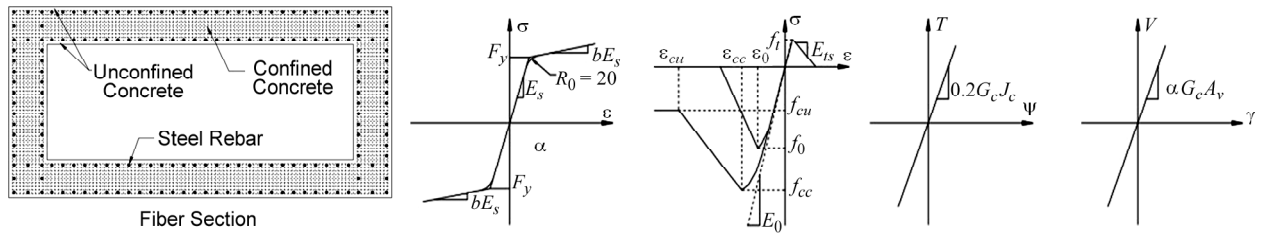**Figure 5.** The numerical skewed bridge model.

Figure 6. Pier fiber cross section and applied constitutive rules.

ear-beam-column elements. Each element consists of three integration points with fiber sections. Steel02 and Concrete02 are used for modeling uniaxial stress-strain relationship of the fibers, according to the available constitutive laws [25-26]. The fiber cross section, uniaxial material models, shear and torsion behavior models are shown in Figure (6).

Results of the pervious experimental and numerical studies [17, 21] have been used to verify the adequacy and accuracy of modeling assumptions of this study by the authors [27]. Figure (7) presents the cyclic relation between base shear and displacement at the top of the scaled pier (1:2.5) with a total height of 8.4 m. Based on this figure, the present numerical model pretty agrees with the experimental results of Pinto et al. [17]. Based on Figure (7) the numerical model prepared by the authors can satisfactory capture pinching behavior of the specimens, comparing with numerical results of Casarotti and Pinho [21].

4.3. Modeling of the Connections

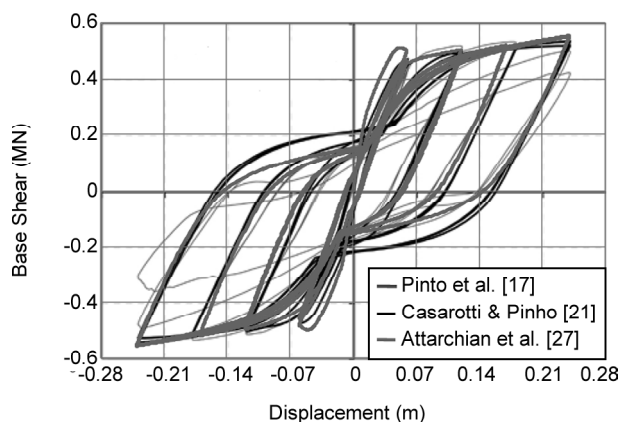The default connection between elements in OpenSees is fixed type. This connection is applied in M models. In order to model seat-type pier-deck connections, an extra node is defined with the same coordination at top of the pier. In P models, the extra node and the node at the top of the pier are constrained to each other only in the transitional degrees of freedom. In this way of modeling, the relative displacement is eliminated, but relative rotation is allowed between deck and pier. In F models, sliding bearing is modeled by flat slider bearing element, a zero length element between the extra node and the bottom node of the rigid element. Figure (5) presents the typical friction sliding bearing and its force-deformation backbone curves. Friction is modeled by Coulomb Friction model in which the variation of kinetic friction coefficient is constant against sliding velocity. According to Priestley et al. [28], for seismic displacement rates, friction coefficient of (PTFE) bearings is predicted to be around 15%.

5. Verifying Dynamic Properties of the Straight Bridge

Modal properties of the models are obtained through Eigenvalue analysis. Dynamic characteristics of the model are compared with those reported by Akbari and Maalek [22] for the bridge with monolithic pier-deck connections (B111) (Table 2). In order to verify the dynamic properties of the presented model, the boundary conditions in abutments are assigned along with the assumptions of Akbari and Maalek. According to Table (2), no significant

Figure 7. Comparing cyclic experimental and numerical results of a 1:2.5 scaled pier [27].

Table 2. Modal properties of the first three transversal modes for B111 and M0 model.

B111-Akbari & Maalek [22]		M0 Model-Present Study	
T (sec)	M^*	T (sec)	M^*
0.216	75.6%	0.213	77%
0.188	0%	0.198	0%
0.157	8%	0.171	9.7%

difference is seen between the modal properties of B111 and those of M0 model. This fact confirms the adequacy of generated model for dynamic analysis.

6. Dynamic Properties of the Skewed Bridges

The results of Eigenvalue analysis for all of the generated models are presented in Tables (3) to (5). Long. and Trans. in Tables (3) to (5) stand for longitudinal and transversal mode shapes, respectively. For all connection types, the first dominant mode shape is torsional. Indeed, straight bridges have similar decoupled mode patterns regardless of the connection types. However, in the skewed bridges mode shapes are coupled including both transversal and longitudinal movements. For all cases as the skew angle increases, the transversal modes become more dominant and the natural period of the system is elongated. The mode shapes are not coupled in the F models due to the lack of internal

restrainers. Concerning the connection types, the flexibility of the bridges increases as the rigidity of the sub- and superstructure connection decreases.

7. Nonlinear Time History Analysis

Bidirectional nonlinear time history analyses have been carried out with seven input ground motions, on the introduced models, according to EC 8 [18]. Ground motions are chosen from the second set of broadband motions introduced by Baker et al. [29] on the rocky sites (Table 6). The records are scaled to the elastic design spectrum (type 1) of soil type B with PGA=0.35g according to EC 8. The resulted scaling factor is 0.5g (Figure 8).

Strong ground motion records are applied along and perpendicular to the bridge alignment, respectively. As shown in Figure (2), major and minor horizontal components of the ground motions are applied along the longitudinal and transversal directions of the bridge, respectively.

Table 3. Modal analysis results in M models.

M0		M15		M30		M45		M60	
Mode	T(sec)	Mode	T(sec)	Mode	T(sec)	Mode	T(sec)	Mode	T(sec)
Torsional	0.427	Torsional	0.423	Torsional	0.413	Torsional	0.394	Torsional	0.378
Trans.	0.216	Trans.-Long.	0.231	Trans.-Long.	0.253	Trans.-Long.	0.280	Trans.	0.328
Long.	0.215	Trans.	0.214	Trans.	0.221	Trans.	0.233	Trans.	0.272
Trans.	0.212	Trans.-Long.	0.205	Trans.	0.203	Trans.-Long.	0.204	Trans.-Long.	0.211
Trans.	0.199	Trans.-Long.	0.198	Long.	0.192	Long.	0.185	Long.	0.177

Table 4. Modal analysis results in P models.

P0		P15		P30		P45		P60	
Mode	T(sec)	Mode	T(sec)	Mode	T(sec)	Mode	T(sec)	Mode	T(sec)
Torsional	0.522	Torsional	0.521	Torsional	0.515	Torsional	0.504	Torsional	0.5
Trans.	0.295	Trans.	0.304	Trans.-Long.	0.320	Trans.-Long.	0.334	Trans.	0.337
Long.	0.250	Long.	0.241	Trans.	0.226	Trans.	0.237	Trans.	0.254
Trans.	0.218	Trans.	0.220	Long.	0.224	Long.- Trans.	0.208	Trans.-Long.	0.210
Trans.	0.201	Trans.	0.202	Trans.-Long.	0.204	Trans.-Long.	0.205	Long.	0.188

Table 5. Modal analysis results in F models.

F0		F15		F30		F45		F60	
Mode	T(sec)	Mode	T(sec)	Mode	T(sec)	Mode	T(sec)	Mode	T(sec)
Torsional	0.524	Torsional	0.522	Torsional	0.518	Torsional	0.513	Torsional	0.509
Trans.	0.335	Trans.	0.340	Trans.	0.351	Trans.	0.357	Trans.	0.442
Long.	0.267	Long.	0.261	Trans.	0.262	Trans.	0.274	Trans.	0.287
Trans.	0.254	Trans.	0.256	Long.	0.250	Long.	0.236	Long.	0.224
Trans.	0.218	Trans.	0.219	Trans.	0.221	Trans.	0.223	Trans.	0.223

Table 6. The characteristics of strong ground motions.

EQ. Name	Year	Station	M	D (km)
San Fernando	1971	Lake Hughes	6.6	25.1
Loma Prieta	1989	Gilroy Array	6.9	18.3
Kocaeli, Turkey	1999	Izmit	7.5	7.2
Northridge	1994	Wonderland	6.7	20.3
Imperial Valley	1979	Cerro Prieto	6.5	15.2
Hector Mine	1999	Hector	7.1	11.7
Duzce, Turkey	1999	Lamont	7.1	8
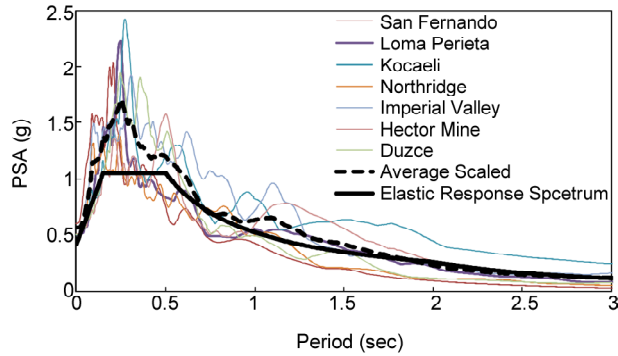
Figure 8. Acceleration Response Spectrum (ARS) of the records scaled to EC8 elastic design spectrum.

8. Results Evaluation

The characteristic of combined loading on the piers is investigated by monitoring several engineering demand parameters of the piers including displacement and force demands. According to Eq. (1), the force demand ratios are obtained from dividing the demand $D_j^i(t)$ by the nominal capacity of the section C_{n-j}. It is to be noted that, j stands for local axis and i is the ground motion label. The maximum absolute ratio corresponding to each ground motion is derived according to Eq. (2). The combined force demand ratios in the time history domain, is computed according to Eq. (3). The maximum absolute value of the combined force demand ratio (Eq. 4) is used to depict better the variation of responses with skew angle.

$$R_{D_j}^i(t) = D_j^i(t)\big/C_{n-j} \qquad (1)$$

$$R_{D_j}^i = \max\left|R_{D_j}^i(t)\right| \qquad (2)$$

$$R_{D_C}^i(t) = \sqrt{[(R_{D_Y}^i(t))^2 + (R_{D_Z}^i(t))^2]} \qquad (3)$$

$$R_{D_C}^i = \max\left|R_{D_C}^i(t)\right| \qquad (4)$$

The mean and one standard deviation of the

selected EDPs are calculated to evaluate the results. In order to investigate the local behavior of plastic hinges, the cross-sectional moment curvature loops are derived. The results are discussed in the following, considering the effect of skew angle and different pier-deck connections.

8.1. Shear Demand on the Piers

Mean and one standard deviation of the maximum shear demand ratios at the base of the piers are derived along the local axes of the pier sections. Nominal shear capacity of the section V_n is estimated according to Caltrans. No significant difference is seen between the trend of force demands of the middle and side piers. Figure (9) shows shear demand ratios at the base of the side piers. Based on Figure (9), though, the demands vary slightly with the skew angle, the trend of shear ratios is contrariwise along the local axes of z and y. The increase of R_{Vz} with the skew angle is probably due to the dominating role of z axis in sustaining the transversal demands, Figure (9a). Based on Figure (9a), R_{Vz} in fixed piers is higher than those in pinned piers, and increases up to 80% of the nominal capacity. The shear ratio demands along minor y axis R_{VY} slightly decrease with the skew angle, Figure (9b). Despite fixity provided in modeling of monolithic piers, fixed piers are in single curvature pattern along y axes, similar to pinned piers. Therefore, as shown in Figure (9b), the shear demand along y axis (R_{Vy}) is quite similar in pinned and fixed piers. In F models, shear demand is limited to the friction force transmitted by bearings and is equal along both local axes. Shear ratio along z axis of F models is twice y axis due to the rectangular shape of pier section, Figures (9a) and (9b).

8.2 Flexural and axial demand on the piers

Moment capacity of the section M_n is determined through moment curvature analysis. Mean and one standard deviation of the maximum moment demand ratios at the base of side piers are presented in Figure (10). The variation of moment ratio demands with skew angle is similar to those of shear demands. Moment demands at the base of the piers of M and P models are greater than yield moment and plastic hinges are formed at the base of the piers. According to values presented in Figure (10), the piers of F models remain elastic. The plastic deformations at
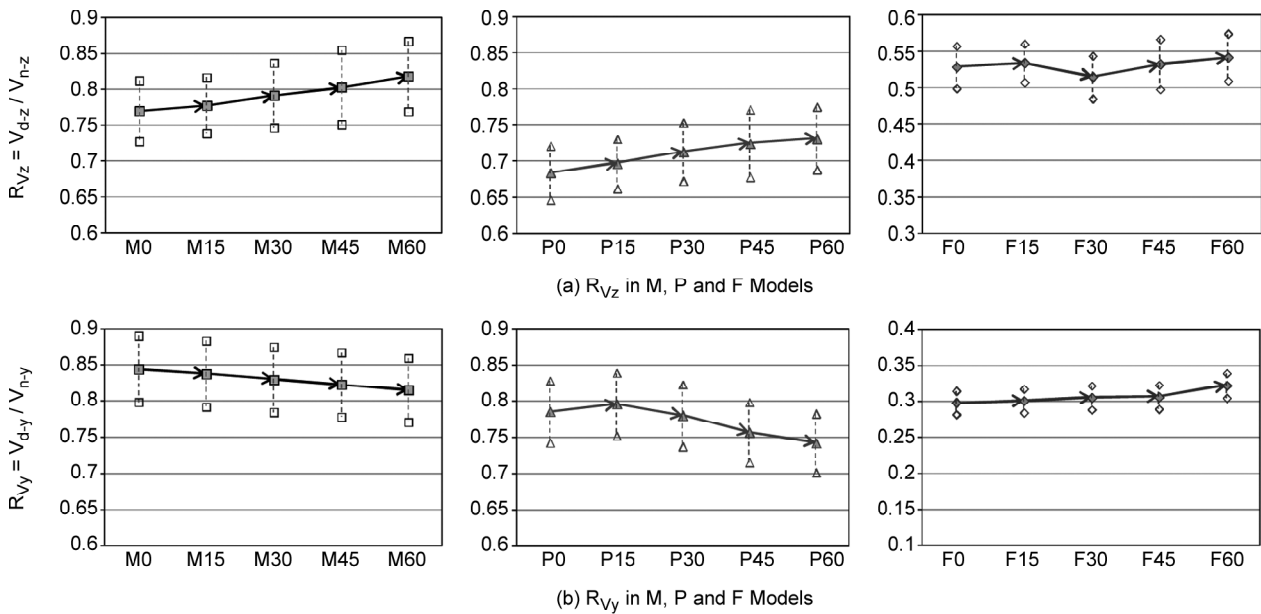
Figure 9. Mean and one standard deviation of shear demand ratios at the base of the side piers.
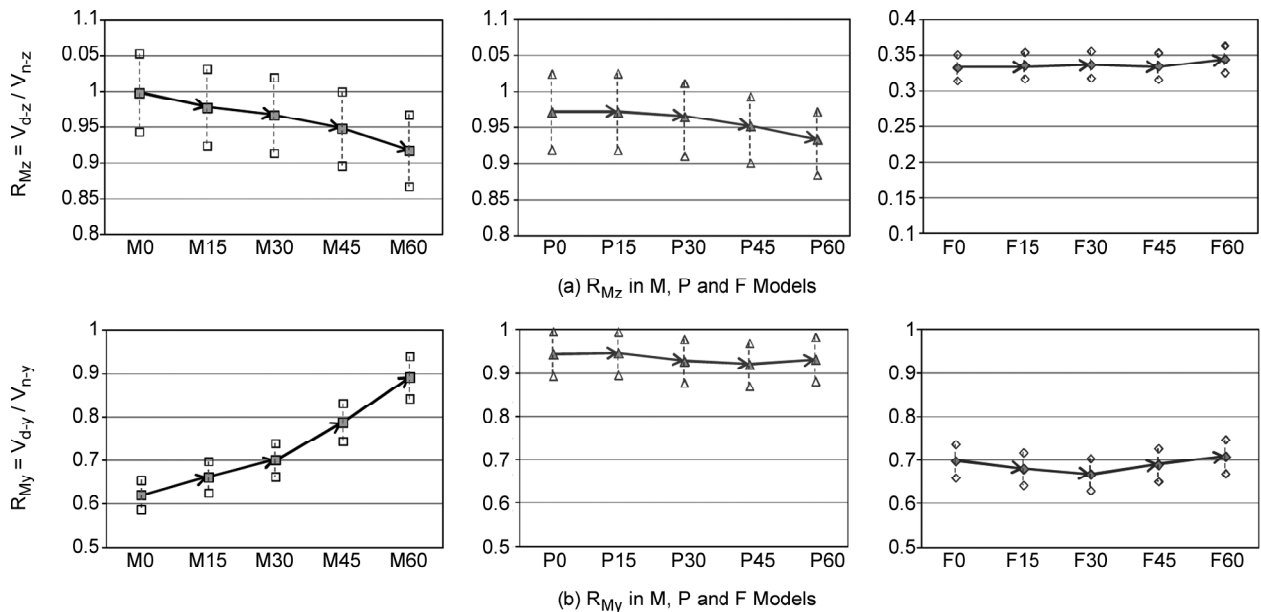

Figure 10. Mean and one standard deviation of moment demand ratios at the base of the side piers.

the base of the piers in M and P models are shown in Figure (11)

In order to get a better understanding of the variation of moment demands with the skew angle, the combined moment ratio R_{M_C} is derived according to Eqs. (3) and (4). Mean and one standard deviation of R_{M_C} at the base of the side piers are presented in Figure (12). Based on Figure (12), moment demands at the base of fixed piers increase with an increase in the skew angle. However, combined moment demand on the piers of P and F

models do not change significantly with the skew angle.

The axial load ratio R_N is presented in Figure (13). No significant variation of the axial demand with the skew angle can be recognized. It should be mentioned that the gravity loading is about 7% of nominal axial capacity N_n of the piers. Axial load is approximately in the gravity load range concerning the piers of F models. However, the piers of P and M models are subjected to 50% additional axial seismic demand due to the interaction between sub- and
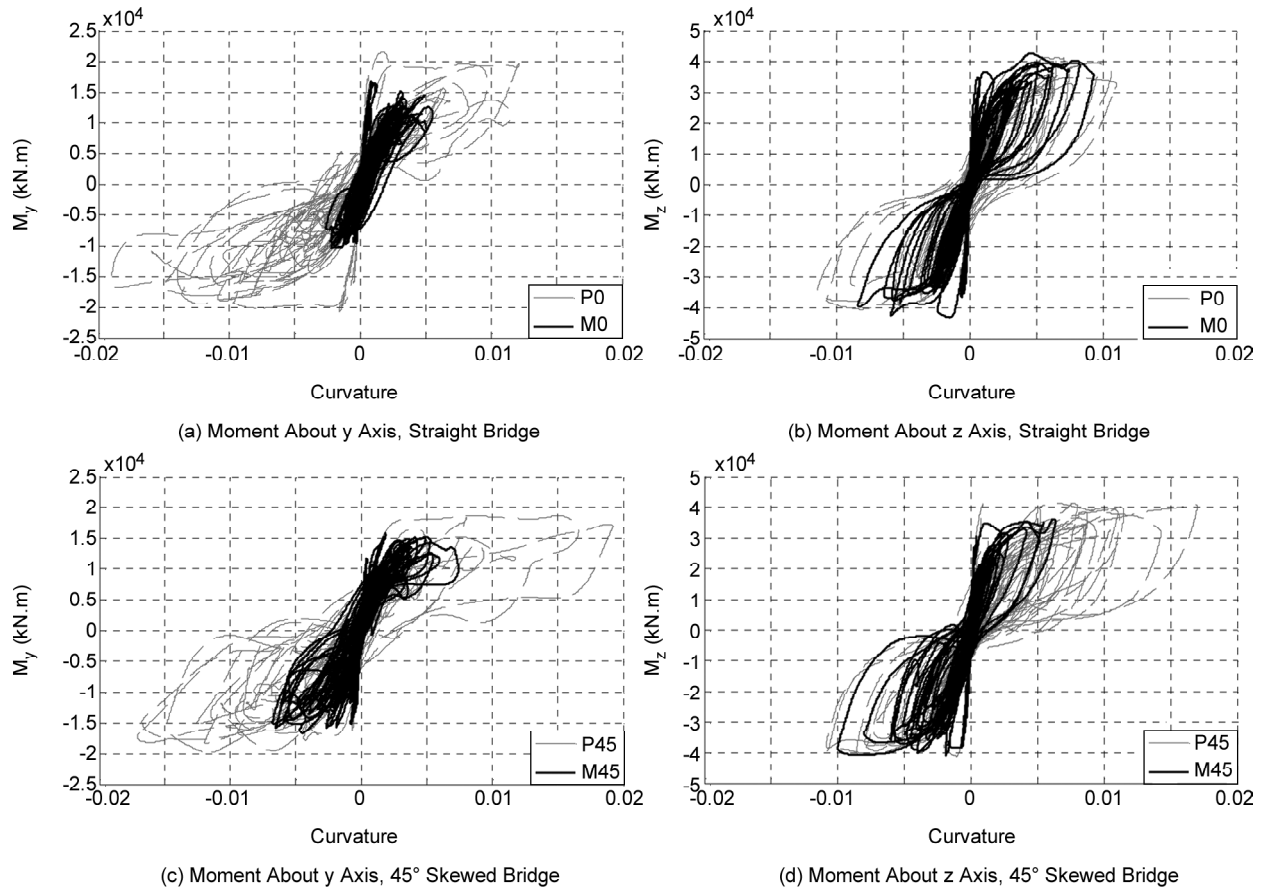
Figure 11. Moment curvature demand at the base of left pier under Imperial Valley earthquake (1979), P: pinned, M: monolithic.
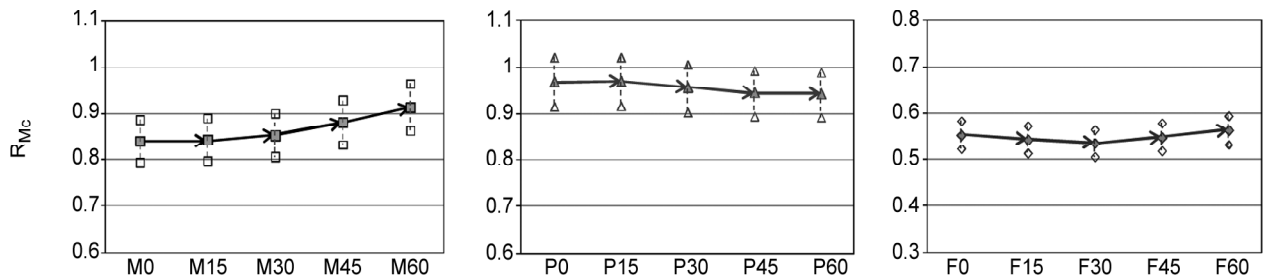

Figure 12. Mean and one standard deviation of R_{Mc} at the base of the side piers.
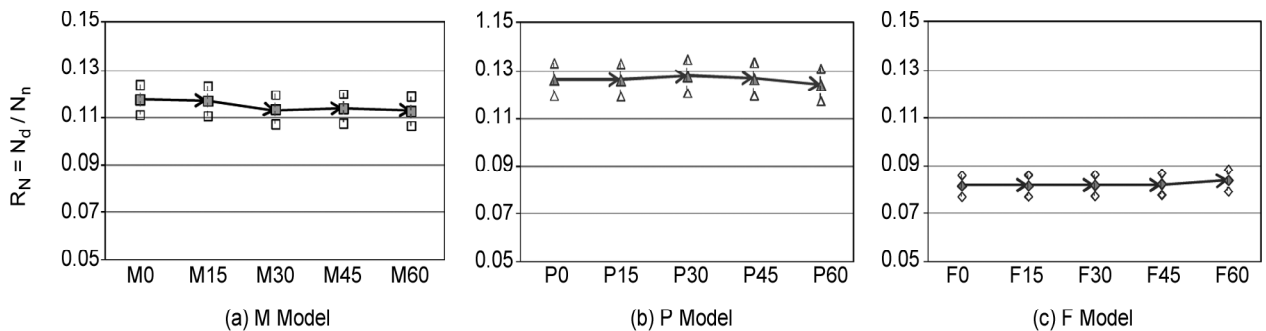

Figure 13. Mean and one standard deviation of R_N at the base of the side piers.

superstructure.

8.3. Torsional Demand on the Piers with Mono-lithic Pier-Deck Connections

Torsional demand of the section T_d is evaluated against cracking torque T_{cr} of the section. The latter is estimated according to AASHTO [30]. Based on the AASHTO, special design and detailing is needed for sections with torques greater than one-quarter of the cracking torque ($T_{cr}/4$). According to AASHTO, the effect of torsion on the flexural capacity and ductility of the section could be ignored, while torsional demand is lesser than one-quarter of the cracking torque. Figure (14) shows the torsional demand ratios on piers with monolithic pier-deck connections. Since rotational degrees of freedom are not restrained in F and P models, there is not any torsional demand on the piers of F and P models. Standard deviations of torsional demands are about 6-9% in the piers. In the single pier bridges, the torsional stiffness is mainly provided by the side piers. As a result of this, torsional demand on the side piers is higher comparing to the middle ones. Figure (14) shows that torsional demand on the piers increases as the skew angle increases. According to Figure (14), torsional demand on side piers is approximately twice the threshold defined in AASHTO. Therefore, side piers should be carefully designed and detailed for required torsional demand. It should be noted that the investigated bridges is a single pier, torsion sensitive bridge. Therefore, for multi column bent bridges, lower torsional demands on fixed piers are anticipated. Concerning the value of combined torsional-flexural loading on the fixed piers, it is sensible to investigate the effect of torsion on the flexural deformation capacity of reinforced sections. According to the findings of this research, the value of torsion in the combined loading studies could be considered between ($T_{cr}/4$) and ($T_{cr}/2$).

8.4. Moment Curvature Demand on the Piers

Moment curvature demand curves are derived for fixed and pinned piers in order to investigate their nonlinear behavior in the plastic hinge regions. As shown in Figure (11), investigated hollow rectangular piers suffer from considerable pinching behavior. This observation is consistent with those reported by Qiang et al. [31-32] in their experimental and numerical researches on hollow rectangular bridge columns. Inelastic deformation demand is significantly higher at the base of piers of P models comparing to that of M models (Figure 11). This fact could be due to the deformation concentration at the bottom of pinned piers. As can be seen in Figure (11), the plastic deformation demand is higher in the 45°-skewed bridges in comparison with that of straight bridges, in both connection types. According to the derived moment curvature curves, it can be concluded that plastic deformation demand of the piers increase with the skew angle.

8.5. Displacement and Rotation Demand of the Deck

Mean transversal displacement demand of the deck Δ_d is shown along the bridge (Figure 15). The standard deviation values are 6-14% for the transversal displacement demand results. Generally, it is anticipated that Δ_d decreases as the rigidity of the pier-deck connection increases. Accordingly, the smallest and largest displacement demands belong to M and F models, respectively (Figure 15). Variation of Δ_d along the bridge is similar to a wide W, due to the elimination of shear keys in the abutments during the modeling. Based on Figure (15), the displacement demand (Δ_d) is quite similar in P and M models, for skew angles less than 30°. However, for the skew angles higher than 30°, the transversal displacement demand in the P models increases steeply with the skew angle. In the F models, the deck has moved considerably over the bearings like a solid element, due to the lack of internal shear keys, Figure (15a). Therefore, deck collapse is quite
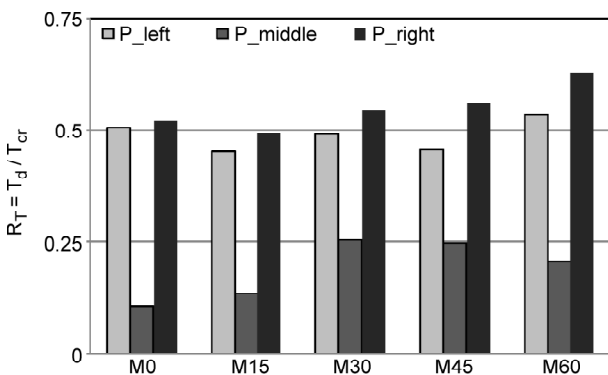

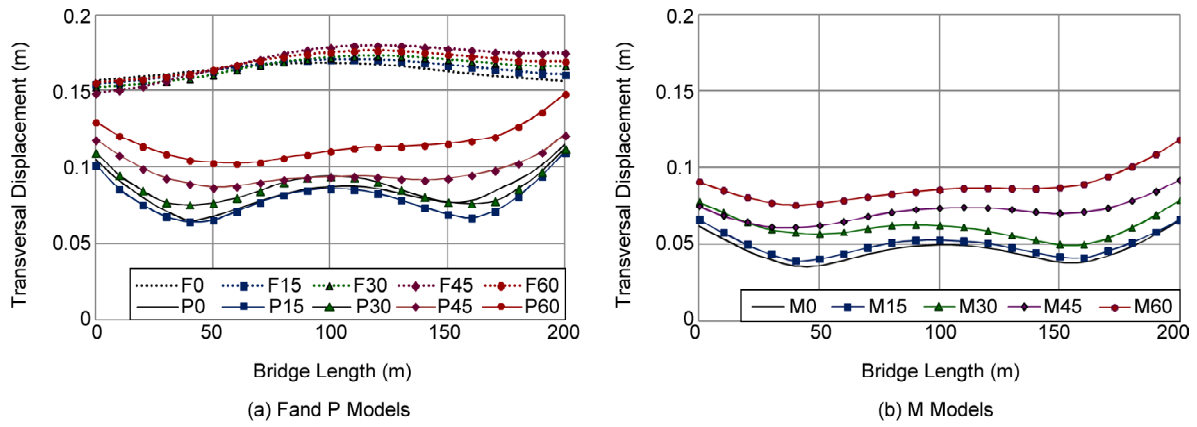**Figure 14.** Mean torsional demand ratios on the piers of M models.

Figure 15. Mean transversal displacement demand along the bridge.

probable in seat-type skewed bridges while shear keys are ineffective. Based on the results presented in Figure (15), it is reasonable to apply seat-type connections in bridges with relatively small skew angles (<30°). In this case, shear keys should be designed to be fully operational. For bridges with skew angles higher than 30°, using monolithic pier-deck connections can diminish and control the displacement demand of the deck.

Figure (16) shows mean and one standard deviation of the rotational demand in the deck. According to this figure, rotational demand increases in all models as the skew angle increases. The rate of this increase steepens in skew angles over 15°. Based on this figure, the rotational demand value is up to 30% lower in M models due to the rigidity of pier-deck connection, comparing to that of P models, Figure (16a) and (16b). The rotational demand has the lowest value in F models due to the uniform solid movement of the deck over the bearings. Comparing the results obtained from P and M models, it can be concluded that the deck can experience considerable rotations regardless the effectiveness of shear keys. Based on the rotational demand values of the deck

in P models, the shear keys are prone to fail in the higher skew angles. The deck collapse probability should be evaluated by combining transversal displacement and rotational demands. In this regard, deck collapse is quite probable in the highly skewed bridges (>30°) with seat-type connections. Consequently, monolithic pier-deck connections are more appropriate for highly skewed bridges.

9. Conclusions

In this study, a torsion sensitive four-span bridge with single-pier bents has been modeled and verified. The skew angles vary from 0° to 60°. Seismic demands of the piers with three different pier-deck connection types are studied conducting bidirectional nonlinear time history analysis in OpenSees. Several engineering demand parameters (EDP) have been evaluated for studying the overall behavior of the bridges. The obtained results are briefly summarized as follows:

❖ The ratio of combined flexural demand on the fixed piers of skewed bridges increases with an increase in the skew angle. However, no significant increase in the amount of combined flexural demand of pinned piers is observed due to the
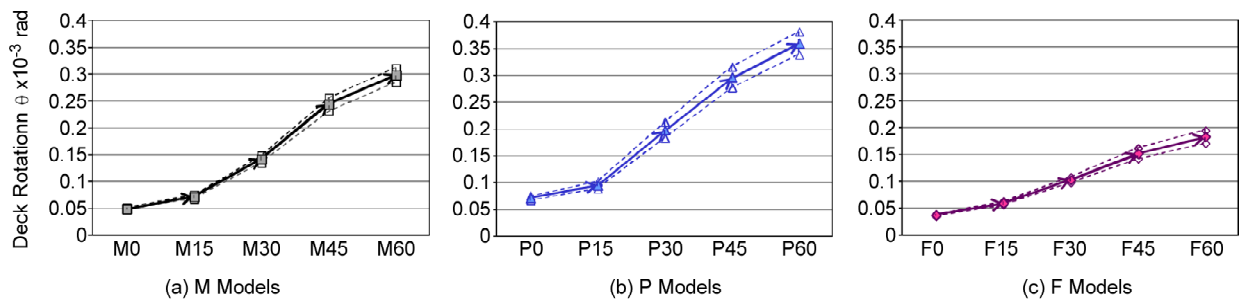

Figure 16. Mean and one standard deviation of rotational demand in the deck.

increase of skew angle.

❖ The torsional demand in the fixed piers is greater than the defined threshold in AASHTO design code. Moreover, its value increases as the skew angle increases. Therefore, fixed piers should be carefully designed and detailed for required torsional demand in the skewed bridges.

❖ Piers of skewed bridges with monolithic pier-deck connections experience combined flexural and torsional loading. The value of combined torsional demand is between $(T_{cr}/4)$ and $(T_{cr}/2)$. These values can be considered in the further studies about the effects of torsional loading on the flexural capacity of reinforced sections.

❖ The ductility demand in pinned piers (P models) is relatively greater than those in fixed piers (M models). This is due to the concentration of plastic deformation at the bottom of pinned piers.

❖ For both pinned and fixed pier-deck connection types, ductility demand of the piers increase with the skew angle.

❖ The movement is quite controlled in the deck of seat-type bridges with skew angles up to 30°, if shear keys are effective and function properly (as assumed in P models). In the larger skew angles (> 30°), the displacement demand increases considerably in the deck of P models. For skew angles larger than 30°, applying monolithic pier-deck connections is more sensible.

❖ In all models, the rotational demand increases with the skew angle. As opposed to P models, the rotational demand decreases up to 30% in the M models by providing rigidity in the pier-deck connections. Therefore, applying monolithic pier-deck connections is more sensible in the highly skewed bridges (>30°).

References

1. Elnashai, A.S., Gencturk, B., Kwon, O.S., Al-Qadi, I., Hashash, Y., Roesler, J.R., Kim, S.J., Jeong, S.H., Dukes, J., and Valdivia, A. (2010) *The Maule (Chile) Earthquake of February 27, 2010, Consequence Assessment and Case Studies*. MAE Center, Report No. 10-04, 208 pp.

2. Zhao, B. and Taucer, F. (2010) Performance of Infrastructure during the May 12, 2008 Wenchuan Earthquake in China. *Journal of Earthquake Engineering*, **14**(4), 578-600.

3. Yen, Ph., Chen, G., Yashinsky, M., Hashash, Y., Holub, C., Wang, K., and Guo, X. (2011a) *China Earthquake Reconnaissance Report: Performance of Transportation Structures During the May 12, 2008, M7.9 Wenchuan Earthquake*. The Federal Highway Administration, Publication No. FHWA-HRT-11-029 Oct, 54 pp.

4. Kawashima, K., Takahashi, Y., Ge, H., Wu, Z., and Zhang, J. (2009) Reconnaissance Report on Damage of Bridges in 2008 Wenchuan, China, Earthquake. *Journal of Earthquake Engineering*, **13**, 965-996.

5. Ghobarah, A.A., and Tso, W.K. (1974) Seismic analysis of skewed highway bridges with intermediate supports. *Earthquake Engineering and Structural Dynamics*, **2**(3), 235-48.

6. Meng, J.Y. and Lui, E.M. (2000) Seismic Analysis and Assessment of a Skew Highway Bridge. *Engineering Structures*, **22**, 1433-1452.

7. Mohti, A.A. and Pekcan, G. (2008) Seismic Response of Skewed RC box-girder Bridges. *Earthquake Engineering and Engineering Vibration*, **7**(4), 415-426.

8. Wilson, T. Mahmoud, H. and Chen, S. (2014) Seismic performance of skewed and curved reinforced concrete bridges in mountainous states. *Engineering Structures*, **70**, 158-167.

9. Deepu, S.P., Prajapat, K., and Chaudhuri, S.R. (2014) Seismic vulnerability of skew bridges under bi-directional ground motions. *Engineering Structures* **71**, 150-160.

10. Hsu, H.L. & Liang L.L. (2003) Performance of hollow composite members subjected to cyclic eccentric loading. *Journal of Earthquake Engineering and Structural dynamics*, **32**, 443-461.

11. Otsuka, H., Takeshita, E., Yabuki, W., Wang, Y., Yoshimura, T., and Tsunomoto, M. (2004) Study on the Seismic Performance of Reinforced Concrete Columns Subjected to Torsional Moment, Bending Moment and Axial Force. *13th World Conference on Earthquake*

Engineering, Vancouver, Paper No. 393.

12. Tirasit, P. and Kawashima, K. (2007) Seismic performance of square RC columns under combined cyclic Flexural and torsional loading. *Journal of Earthquake Engineering*, **11**, 425-452.

13. Li, Q., Belarbi, A., and Prakash, S.S. (2010) Seismic Performance of square RC Bridge Columns under Combined loading including torsion with low shear. Paper No. 3011, *Proceedings of the Earth and Space 2010 Conference: Engineering, Science, Construction and Operations in Challenging Enviroments*. ASCE 2010.

14. Prakash S.S. (2009) *Seismic Behavior of Circular RC bridge Columns under Combined Loading Including Torsion*. Ph.D. Dissertation, Department of Civil and Environmental Engineering, University of Houston, 316 pp.

15. Prakash, S.S., Belarbi, A., and You, Y.M. (2010) Seismic Performance of Circular RC Columns Subjected to Axial, Bending, and Torsion with Low and Moderate Shear. *Journal of Engineering Structures*, Elsevier, **32**(1), 46-59.

16. OpenSees (2008) *OpenSees Development Team, Open System for Earthquake Engineering Simulations*, Version 2.3.0, [online]. Available from: http://opensees.berkeley.edu.

17. Pinto, A.V., Verzeletti, G., Pegon, P., Magonetto, G., Negro, P., and Guedes, J. (1996) *Pseudo-Dynamic and shaking table tests on RC bridges ECOEST-PrEC8*. Report No.5, Brussels.

18. CEN European Committee for Normalization, Eurocode 8 (2005) *Design of Structures for Earthquake Resistance - Part 2; Bridges*, EN 1998-2.

19. Kappos, A.J., Manolis, G.D., and Moschonas, I.F. (2002) Seismic Assessment and design of R/C bridges with irregular configuration, including SSI effects. *Engineering Structures*, **24**, 1337-1348.

20. Isakovic, T., Lazaro, M., and Fischinger, M. (2008) Applicability of pushover methods for the seismic analysis of single column bent viaducts. *Earthquake Engineering & Structural Dynamics*, **37**, 1185-1202.

21. Casarotti, Ch., and Pinho, R. (2006) Seismic response of continuous span bridges through fiber-based finite element analysis. *Earthquake Engineering and Engineering Vibration*, **5**, 119-131.

22. Akbari, R. and Maalek, Sh. (2010) Adequacy of the seismic analysis method for single-column-bent viaducts considering regularity and higher modes effects. *Journal of Vibration and Control*, **16**, 827-852.

23. Aviram, A., Mackie, K.R., and Stojadinovic, B. (2008) *Guidelines for Nonlinear Analysis of Bridge Structures in California*. PEER Report. 2008/03.

24. Caltrans SDC (2010) *Caltrans Seismic Design Criteria Version 1.6*. California Department of Transportation, Sacramento.

25. Menegotto, M. and Pinto, P.E. (1973) 'Method of Analysis for Cyclically Loaded R.C. Plane Frames Including Changes in Geometry and Non-elastic Behavior of Elements under Combined Normal Force and Bending'. In: *Symposium on the Resistance and Ultimate Deformability of structures Acted on by Well Defined Repeated Loads*, International Association for Bridge and Structural Engineering, Zurich, Switzerland. Lisbon: IABSE Report, Vol. 13, Final Report, 15-22.

26. Mander, J.B., Priestley, M.J.N., and Park, R. (1988) Theoretical Stress-strain Model for confined Concrete. *Journal of Structural Engineering*, ASCE, **114**, 1804-1826.

27. Attarchain, N., Kalantari, A., and Moghaddam, A.S. (2013) Cyclic Behavior Modeling of Rectangular RC Bridge Piers Using OpenSees. *Proceedings of the 4th ECCOMAS Thematic Conference on Computational Methods in Structural Dynamics and Earthquake Engineering, COMPDYN 2013*. Kos Island, Greece, 12-14 June.

28. Priestley, M.J.N., Seible, F., and Calvi, G.M.

(1996) *Seismic Design and Retrofit of Bridges.* New York, NY, Wiley.

29. Baker, J.W., Lin, T., Shahi, S.K., and Jayaram, N. (2011) *New Ground Motion Selection Procedures and Selected Motions for the PEER Transportation Research Program.* PEER Report 2011/03.

30. AASHTO (2012) *AASHTO LRFD Bridge Design Specification.* American Association of State Highway and Transportation Officials.

31. Qiang, H., Xiuli, D., Zhou, Y., and Lee, G.C. (2013) Experimental study of hollow rectangular bridge column performance under vertical and cyclically bilateral loads. *Earthquake Engineering and Engineering Vibration*, **12**(3), 433-445.

32. Qiang, H., Yulong, Z., Xiuli, D., Chao, H., and George, C.L. (2014) Experimental and numerical studies on seismic performance of hollow RC bridge columns. *Earthquakes and Structures*, **7**(3), 251-265.